Published in final edited form as:

Int J Cardiovasc Imaging. 2016 March ; 32(3): 461–467. doi:10.1007/s10554-015-0792-x.

Blood Flow Characteristics in the Ascending Aorta after TAVI compared to Surgical Aortic Valve Replacement

Ralf Felix Trauzeddel[*], **Ulrike Löbe, MD**[†], **Alex J Barker, PhD**[‡,§], **Carmen Gelsinger, MD**[†], **Christian Butter, MD**[†], **Michael Markl, PhD**[‡,§], **Jeanette Schulz-Menger, MD**[*], and **Florian von Knobelsdorff-Brenkenhoff, MD**[*]

[*]Working Group Cardiovascular Magnetic Resonance, Experimental and Clinical Research Center, a joint cooperation between the Charité Medical Faculty and the Max-Delbrueck Center for Molecular Medicine; and HELIOS Klinikum Berlin Buch, Department of Cardiology and Nephrology, Berlin, Germany

[†]Immanuel Klinikum Bernau Heart Center Brandenburg, Department of Cardiology, Bernau, Germany

[‡]Department of Radiology, Feinberg School of Medicine, Northwestern University, Chicago, IL, USA

[§]Department of Biomedical Engineering, McCormick School of Engineering, Northwestern University, Chicago, IL, USA

Abstract

Purpose—Ascending aortic blood flow characteristics are altered after aortic valve surgery, but the effect of transcatheter aortic valve implantation (TAVI) is unknown. Abnormal flow may be associated with aortic and cardiac remodeling. We analyzed blood flow characteristics in the ascending aorta after TAVI in comparison to conventional stented aortic bioprostheses (AVR) and healthy subjects using time-resolved three-dimensional flow-sensitive cardiovascular magnetic resonance imaging (4D-flow MRI)

Methods—Seventeen patients with TAVI (Edwards Sapien XT), 12 with AVR and 9 healthy controls underwent 4D-flow MR (spatial / temporal resolution $2.1\times2.4\times2.2mm^3$ / 38.4ms) of the ascending aorta. Target parameters were: severity of vortices and helices (semiquantitative grading from 0=none to 3=severe) and the local distribution of systolic wall shear stress ($WSS_{systole}$).

Results—AVR revealed significantly more extensive vortices and helices than TAVI ($p=0.042$ and $p=0.002$) and controls ($p<0.001$ and $p=0.001$). TAVI showed significantly more extensive vortices than controls ($p<0.001$). Both TAVI and AVR revealed marked blood flow eccentricity

Address for correspondence: Florian von Knobelsdorff-Brenkenhoff; Working Group Cardiovascular Magnetic Resonance; Charité Medical University Berlin, Experimental and Clinical Research Center, Lindenberger Weg 80, 13125 Berlin, Germany; Tel. +49 30 450 540615, Fax +49 30 450 540915, ; Email: florian.von-knobelsdorff@charite.de

Conflict of Interest: The authors declare that they have no conflict of interest.

Compliance with Ethical Standards

All human studies have been approved by the local ethics committees and have therefore been performed in accordance with the ethical standards laid down in the 1964 Declaration of Helsinki and its later amendments. All persons gave their informed consent prior to their inclusion in the study.

(64.7% and 66.7%, respectively), whereas controls showed central blood flow (88.9%). TAVI and AVR exhibited an asymmetric distribution of $WSS_{systole}$ in the mid-ascending aorta with local maxima at the right anterior aortic wall and local minima at the left posterior wall. In contrast, controls showed a symmetric distribution of $WSS_{systole}$ along the aortic circumference.

Conclusions—Blood flow was significantly altered in the ascending aorta after TAVI and AVR. Changes were similar regarding $WSS_{systole}$ distribution, while TAVI resulted in less helical and vertical blood flow.

Keywords

magnetic resonance imaging; aorta; aortic valve replacement; shear stress; transcatheter aortic valve implantation; 4D-flow

Introduction

Transcatheter aortic valve implantation (TAVI) has become an accepted method for treating patients with severe aortic stenosis who are not eligible or at high risk for conventional surgical aortic valve replacement (AVR) [1-3]. Previous studies have demonstrated that changes in the geometry of the aortic valve such as bicuspid valves or AVR result in altered blood flow patterns and parameters [4,5]. These abnormalities may be associated with aortic remodeling and increased cardiac afterload [6,7].. As there is little knowledge about the effect of TAVI on the global patterns of blood flow in the ascending aorta, the aim of this study was to analyze the blood flow characteristics in the ascending aorta after TAVI in comparison to AVR with a stented aortic bioprosthesis and healthy controls using time-resolved, three-dimensional, flow-sensitive magnetic resonance (4D-flow MRI). This technique allows for the visualization of complex blood flow in the form of helices and vortices as well as quantifying local flow velocities and WSS [8]. We hypothesize that both AVR and TAVI will result in altered hemodynamics compared to controls.

Materials and Methods

Study sample

The local ethics committee approved the study. Written informed consent was obtained from all individuals. Twenty-three consecutive patients with TAVI with an Edwards Sapien XT® prosthesis were prospectively enrolled. This study focused on the Edwards Sapien XT® as at the time of study enrollment this was the preferred device in the cooperating TAVI center. The data of 12 patients with stented bioprostheses and 9 healthy controls were retrospectively analyzed from a previous study [5]. The characteristics of the study participants are summarized in Table 1.

Image acquisition protocol

Images were acquired as previously described [5]. All subjects underwent a CMR examination at a 1.5 Tesla MR scanner (Magnetom Avanto, Siemens Healthcare, Erlangen, Germany). A 12-channel anterior body array coil was used for signal reception and the body coil for signal transmission. 4D-flow was acquired using a sagittal oblique volume covering

the thoracic aorta. Prospective ECG gating was used with a respirator navigator placed on the lung-liver interface. The following scan parameters were chosen: echo time [TE] = 2.3 ms, repetition time [TR] = 4.8 ms, bandwith = 440 Hz/pixel, acceleration mode GRAPPA with factor 2 to 5, reference lines = 24, flip angle $\alpha = 9°$, temporal resolution = 38.4 ms, field of view = 400 × 375 mm, matrix = 192 × 158, voxel size = 2.1 × 2.4 × 2.2 mm^3, phase encoding direction = anterior-posterior, number of slices = 12 - 26, velocity encoding = 1.5 - 2.5 m/s.

Conventional ECG-gated, breath-held steady-state free-precession (SSFP) cine imaging was performed to quantify left ventricular function and the orifice area of the aortic valve and bioprostheses, respectively [9]. The effective orifice area (EOA) of TAVI could not be determined from SSFP images due to significant artefacts, but was taken from the literature [10,11]. Axial SSFP still images of the thorax were used to estimate the size of the ascending aorta at the level of the pulmonary bifurcation [12].

Processing and analysis of the images

All 4D-flow MRI data were processed as previously described [8]. Briefly, data were corrected for noise, eddy currents and velocity aliasing (MatLab; The MathWorks, Natick, MA, USA) [13]. In a second step, a 3D phase contrast MR angiogram was calculated based on the flow measurements to position the analysis planes and to visualize the blood flow (EnSight, CEI, Apex, NC). Three planes were positioned perpendicular to the longitudinal axis of the aortic wall: at the level of the sinotubular junction (S1), in the ascending aorta at the level of the pulmonary bifurcation (S2), and proximal to the brachiocephalic trunk (S3), as recommended in the literature [14] and previously shown [5]. The position of S1 was selected such that it was high enough to avoid signal artifact caused by the presence the metal in the prosthetic stents. These analysis planes were exported into previously reported software for the segmentation and calculation of the blood flow parameters (MatLab; The MathWorks, Natick, MA, USA) [13].

Left ventricular function quantification and planimetry of the orifice area were achieved by manual segmentation using commercial software (CVI42, Circle Cardiovascular Imaging, Calgary, Canada). Assessment of the aortic diameter was done at the in ascending aorta at the level of the pulmonary bifurcation [12].

Blood flow helicity and vorticity in the ascending aorta

Blood flow patterns were semi-quantitatively evaluated using pathline movies and classified as vortex and helix formation as previously described [5]. In short, helices and vortices were graded in 4 categories: 0 = none, 1 = mild, 2 = moderate, 3 = severe at the mid-ascending aorta [5].

Blood flow eccentricity in the ascending aorta

Blood flow was semi-quantitatively graded as central or mild eccentric or marked eccentric as previously described [5,15]. A central flow was characterized if the flow occupied the majority of the vessel lumen. A mild eccentric flow occupied two-thirds to one-third of the vessel and a marked eccentric flow occupied one-third or less of the vessel.

Wall shear stress in the ascending aorta

Quantification of systolic WSS ($WSS_{systole}$; unit N/m^2) was performed for 8 regional segments along the aortic circumference for each analysis plane S1-S3 as previously described [17]. Regional WSS was averaged over three time points.

Statistical analysis

Analysis of the data was performed using SPSS 22 (IBM, Armonk, US). Graphics were created using PRISM 5 (GraphPad Software Inc, San Diego, California, US) and plug-in software for MatLab. Categorical data are expressed as percentages, continuous data as mean ± standard deviation (SD). The three groups (TAVI, AVR, controls) were compared using a Kruskal-Wallis test. $WSS_{systole}$ was tested on a regional basis for significance using a paired two-tailed t-test for equal or unequal variances (depending on a two sample F-test). In case of significance, a Mann-Whitney-U test was added. Statistical significance was set at a probability level of < 0.05.

Results

Baseline characteristics

Table 1 summarizes the baseline characteristics of the study participants. Six patients were excluded from further analysis due to extensive respiratory motion and thus inefficient respiratory navigator. Healthy controls were significantly younger than patients with AVR ($p=0.002$) and TAVI ($p=0.001$) and had significantly larger EOA ($p<0.001$) and EOA index ($p<0.001$). They also had a smaller aortic diameter than AVR ($p=0.003$) and TAVI ($p=0.021$). AVR and TAVI were not different regarding age ($p = 0.347$), but AVR hat larger aortic diameter ($p=0.018$) and TAVI had larger EOA ($p=0.027$), but did not differ significantly from AVR regarding the EOA index ($p=0.060$).

Blood flow patterns

All examinations resulted in diagnostic image quality. Local artifacts occurred in the proximity of the prosthetic stents similarly for TAVI and AVR. The most proximal analysis plane was therefore positioned at the sinotubular level to warrant sufficient distance from the artifact. Representative blood flow patterns of the three groups are shown in figure 1. Figure 2 shows a comparison between the qualitative grades for vortex and helix severity. AVR revealed significantly more severe helices and vortices than TAVI and controls, whereas TAVI only had significant more vortices, but not helices, than normal subjects.

Blood flow eccentricity

Figure 3 summarizes the grading of the blood flow eccentricity. Controls predominantly exhibited central flow. In contrast, 11/17 TAVI patients had a markedly eccentric flow and the remaining 6 showed mildly eccentric flow. Similarly, 8/12 AVR recipients had markedly eccentric flow and the remaining 4 were mildly eccentric. AVR and TAVI differed significantly concerning the mean value of eccentricity from healthy subjects ($p<0.001$). TAVI and AVR did not differ significantly ($p = 0.777$)

Wall shear stress

The distribution of $WSS_{systole}$ in the ascending aorta is illustrated in figure 4. Compared to controls, TAVI revealed significantly higher $WSS_{systole}$ at the right anterior segment at the mid-ascending aorta, and significantly lower WSS at the mid-ascending aorta and distal ascending aorta in the right-posterior, posterior, left-posterior and left segments. Similarly, AVR showed significantly lower $WSS_{systole}$ compared to healthy controls at the posterior segments at S2 and S3 and at the left segment at S1. At the right anterior segment at the mid-ascending aorta, AVR showed elevated $WSS_{systole}$ compared to healthy controls but which were not statistically significant. TAVI and AVR did not differ significantly regarding WSS_{peak} in all analysis planes.

Discussion

In this pilot study, we used 4D-flow MRI to assess the blood flow in the ascending aorta after TAVI in comparison to AVR with stented bioprostheses as well as healthy controls. TAVI and AVR revealed significantly higher regional blood flow patterns in the form of helices and vortices as well as $WSS_{systole}$ and a more eccentric blood flow than controls.

Both stented bioprostheses and TAVI consist of biological material mounted on a stent. Despite this similarity, AVR resulted in more distinct helices and vortices than TAVI. This may be attributed to the lower EOA of the AVR cohort in this study, but may also reflect differences in stent design. Whereas the TAVI device is fixed passively at the calcified aorta wall, stented bioprostheses contain a sewing ring that may be an unfavorable obstacle within the blood flow, even if the implantation is done principally completely supra-annularly. The latter aspect is supported by generally lower pressure gradients of TAVI compared to AVR reported in the literature [18,19]. Despite this potential advantage of TAVI, TAVI - as expected - also led to an abnormal blood flow pattern compared to healthy controls. At least for bicuspid aortic valves, a correlation of blood flow pattern and aortic growth rate has been shown [6]. Furthermore, novel studies that link blood flow pattern to energy loss suppose an association of blood flow pattern and cardiac afterload [20,7]. Hence, future studies have to evaluate whether the altered blood flow of TAVI and AVR has impact on aortic and left ventricular remodeling as well. Both TAVI and stented bioprostheses revealed an eccentric distribution of blood flow velocities in the ascending aorta compared to healthy controls, who exhibited a physiological central flow. An eccentric flow is associated with regional elevation of WSS [4,20,6]. This is hypothesized to contribute to an increase of the aortic diameter and aneurysm formation [21] and may be associated with a increased viscous and turbulent energy losses [7,20]. TAVI and AVR revealed a similar eccentric distribution of WSS along the aortic circumference, which was significantly elevated and depressed in focal regions. This asymmetry clearly differed from healthy controls. Local abnormalities in WSS are thought to stimulate aneurysm formation [22,23]. In a recent study using computational fluid-dynamic analysis, WSS has been shown to be regionally elevated at the site of ascending aortic aneurysm formation [24]. Furthermore, studies reported that the WSS reached a critical value at aneurysm diameters of 6cm [25] - a cutoff, which is known be associated with a high risk of aortic dissection. Hence, it is notable that both TAVI and AVR lead to a WSS profile that imparts a regional hemodynamic abnormality at the aortic wall,

which is suspected to increase the chance of an adverse vascular event. Whether the resultant WSS patterns are relevant for patients with calcified aortic stenosis, who typically have thickened and stiff aortic walls, is unclear. However, in patients with aortic regurgitation and thinned aortic wall, who may receive AVR or even TAVI in the future, this prior knowledge regarding the impact of AVR and TAVI may prove useful.

Limitations

i) The control group differed from the intervention groups regarding age, orifice area and aortic dimensions. Age has a known influence on the hemodynamics in the ascending aorta as well as the aortic diameter [26–28]. Therefore, this study has to be interpreted as a pilot study. ii) It is known that 4D-flow underestimates the true WSS [24]. However, as we chose the same technique in all subjects, the relative differences are comparable. iii) The orifice area of the TAVI prostheses was taken from literature, as direct measurement was infeasible due to artifacts. iv) This cross-sectional study was designed as a hypothesis generating pilot study, thus the enrollment was limited to small numbers. To examine the influence of the blood flow characteristics on the ascending aorta, a longitudinal study is required.

Conclusion

This pilot study demonstrated that TAVI and AVR with a stented bioprosthesis lead to altered blood flow characteristics in the ascending aorta compared to healthy controls, with more intense flow eccentricity and regional elevation of wall shear stress.

Acknowledgements

We thank our technicians Kerstin Kretschel, Evelyn Polzin and Denise Kleindiest for performing the CMR scans. We also thank our study nurses Elke Nickel-Szczech and Annette Koehler as well as the other working group members for their assistance in realizing the study.

Funding: This study was partly funded by the National Institutes of Health (NIH K25HL119608, R01HL115828)

Abbreviations

EOA	Effective orifice area
AVR	aortic valve replacement
SD	Standard deviation
SSFP	steady-state free-precession
TAVI	Transcatheter aortic valve implantation
WSS	Wall shear stress
4D-flow	Time-resolved three-dimensional flow-sensitive cardiovascular magnetic resonance imaging

References

1. Cribier A. Percutaneous Transcatheter Implantation of an Aortic Valve Prosthesis for Calcific Aortic Stenosis: First Human Case Description. Circulation. 2002; 106(24):3006–3008. doi:10.1161/01.cir.0000047200.36165.b8. [PubMed: 12473543]
2. Leon MB, Smith CR, Mack M, Miller DC, Moses JW, Svensson LG, Tuzcu EM, Webb JG, Fontana GP, Makkar RR, Brown DL, Block PC, Guyton RA, Pichard AD, Bavaria JE, Herrmann HC, Douglas PS, Petersen JL, Akin JJ, Anderson WN, Wang D, Pocock S, PARTNER Trial Investigators. Transcatheter Aortic-Valve Implantation for Aortic Stenosis in Patients Who Cannot Undergo Surgery. N Engl J Med. 2010; 363(17):1597–1607. doi: 10.1056/NEJMoa1008232. [PubMed: 20961243]
3. Smith CR, Leon MB, Mack MJ, Miller DC, Moses JW, Svensson LG, Tuzcu EM, Webb JG, Fontana GP, Makkar RR, Williams M, Dewey T, Kapadia S, Babaliaros V, Thourani VH, Corso P, Pichard AD, Bavaria JE, Herrmann HC, Akin JJ, Anderson WN, Wang D, Pocock SJ, PARTNER Trial Investigators. Transcatheter versus Surgical Aortic-Valve Replacement in High-Risk Patients. N Engl J Med. 2011; 364(23):2187–2198. doi: 10.1056/NEJMoa1103510. [PubMed: 21639811]
4. Barker AJ, Markl M, Burk J, Lorenz R, Bock J, Bauer S, Schulz-Menger J, von Knobelsdorff-Brenkenhoff F. Bicuspid aortic valve is associated with altered wall shear stress in the ascending aorta. Circ Cardiovasc Imaging. 2012; 5(4):457–466. doi:10.1161/CIRCIMAGING.112.973370. [PubMed: 22730420]
5. von Knobelsdorff-Brenkenhoff F, Trauzeddel RF, Barker AJ, Gruettner H, Markl M, Schulz-Menger J. Blood flow characteristics in the ascending aorta after aortic valve replacement-a pilot study using 4D-flow MRI. International journal of cardiology. 2014; 170(3):426–433. doi:10.1016/j.ijcard.2013.11.034. [PubMed: 24315151]
6. Hope MD, Wrenn J, Sigovan M, Foster E, Tseng EE, Saloner D. Imaging biomarkers of aortic disease: increased growth rates with eccentric systolic flow. J Am Coll Cardiol. 2012; 60(4):356–357. doi:10.1016/j.jacc.2012.01.072. [PubMed: 22813616]
7. Barker AJ, van Ooij P, Bandi K, Garcia J, Albaghdadi M, McCarthy P, Bonow RO, Carr J, Collins J, Malaisrie SC, Markl M. Viscous energy loss in the presence of abnormal aortic flow. Magn Reson Med. 2014; 72(3):620–628. doi:10.1002/mrm.24962. [PubMed: 24122967]
8. Markl M, Frydrychowicz A, Kozerke S, Hope M, Wieben O. 4D flow MRI. J Magn Reson Imaging. 2012; 36(5):1015–1036. doi:10.1002/jmri.23632. [PubMed: 23090914]
9. Schulz-Menger J, Bluemke DA, Bremerich J, Flamm SD, Fogel MA, Friedrich MG, Kim RJ, von Knobelsdorff-Brenkenhoff F, Kramer CM, Pennell DJ, Plein S, Nagel E. Standardized image interpretation and post processing in cardiovascular magnetic resonance: Society for Cardiovascular Magnetic Resonance (SCMR) Board of Trustees Task Force on Standardized Post Processing. Journal of Cardiovascular Magnetic Resonance. 2013; 15(35):1–19. doi: 10.1186/1532-429X-15-35. [PubMed: 23324167]
10. Spethmann S, Dreger H, Schattke S, Baldenhofer G, Saghabalyan D, Stangl V, Laule M, Baumann G, Stangl K, Knebel F. Doppler haemodynamics and effective orifice areas of Edwards SAPIEN and CoreValve transcatheter aortic valves. Eur Heart J Cardiovasc Imaging. 2012; 13(8):690–696. doi:10.1093/ehjci/jes021. [PubMed: 22307868]
11. Binder RK, Webb JG, Toggweiler S, Freeman M, Barbanti M, Willson AB, Alhassan D, Hague CJ, Wood DA, Leipsic J. Impact of post-implant SAPIEN XT geometry and position on conduction disturbances, hemodynamic performance, and paravalvular regurgitation. JACC Cardiovasc Interv. 2013; 6(5):462–468. doi:10.1016/j.jcin.2012.12.128. [PubMed: 23702010]
12. von Knobelsdorff-Brenkenhoff F, Rudolph A, Wassmuth R, Abdel-Aty H, Schulz-Menger J. Aortic dilatation in patients with prosthetic aortic valve: comparison of MRI and echocardiography. J Heart Valve Dis. 2010; 19(3):349–356. [PubMed: 20583398]
13. Stalder AF, Russe MF, Frydrychowicz A, Bock J, Hennig J, Markl M. Quantitative 2D and 3D phase contrast MRI: optimized analysis of blood flow and vessel wall parameters. Magn Reson Med. 2008; 60(5):1218–1231. doi:10.1002/mrm.21778. [PubMed: 18956416]
14. Hiratzka LF, Bakris GL, Beckman JA, Bersin RM, Carr VF, Casey DE Jr. Eagle KA, Hermann LK, Isselbacher EM, Kazerooni EA, Kouchoukos NT, Lytle BW, Milewicz DM, Reich DL, Sen S, Shinn JA, Svensson LG, Williams DM. 2010 ACCF/AHA/AATS/ACR/ASA/SCA/

SCAI/SIR/STS/SVM Guidelines for the diagnosis and management of patients with thoracic aortic disease: Executive summary: A report of the American College of Cardiology Foundation/American Heart Association Task Force on Practice Guidelines, American Association for Thoracic Surgery, American College of Radiology, American Stroke Association, Society of Cardiovascular Anesthesiologists, Society for Cardiovascular Angiography and Interventions, Society of Interventional Radiology, Society of Thoracic Surgeons, and Society for Vascular Medicine. Anesth Analg. 2010; 111(2):279–315. doi:10.1213/ANE.0b013e3181dd869b. [PubMed: 20664093]

15. Hope MD, Hope TA, Crook SE, Ordovas KG, Urbania TH, Alley MT, Higgins CB. 4D Flow CMR in Assessment of Valve-Related Ascending Aortic Disease. JACC Cardiovasc Imaging. 2011; 4(7): 781–787. doi:10.1016/j.jcmg.2011.05.004. [PubMed: 21757170]
16. Mahadevia R, Barker AJ, Schnell S, Entezari P, Kansal P, Fedak PW, Malaisrie SC, McCarthy P, Collins J, Carr J, Markl M. Bicuspid Aortic Cusp Fusion Morphology Alters Aortic 3D Outflow Patterns, Wall Shear Stress and Expression of Aortopathy. Circulation. 2013 doi:10.1161/CIRCULATIONAHA.113.003026.
17. Barker AJ, Markl M, Bürk J, Lorenz R, Bock J, Bauer S, Schulz-Menger J, von Knobelsdorff-Brenkenhoff F. Bicuspid Aortic Valve is Associated with Altered Wall Shear Stress in the Ascending Aorta. Circ Cardiovasc Imaging. 2011; 5(4):457–66. doi: 10.1161/CIRCIMAGING.112.973370. [PubMed: 22730420]
18. Clavel MA, Webb JG, Rodes-Cabau J, Masson JB, Dumont E, De Larochelliere R, Doyle D, Bergeron S, Baumgartner H, Burwash IG, Dumesnil JG, Mundigler G, Moss R, Kempny A, Bagur R, Bergler-Klein J, Gurvitch R, Mathieu P, Pibarot P. Comparison between transcatheter and surgical prosthetic valve implantation in patients with severe aortic stenosis and reduced left ventricular ejection fraction. Circulation. 2010; 122(19):1928–1936. doi:10.1161/CIRCULATIONAHA.109.929893. [PubMed: 20975002]
19. Fairbairn TA, Steadman CD, Mather AN, Motwani M, Blackman DJ, Plein S, McCann GP, Greenwood JP. Assessment of valve haemodynamics, reverse ventricular remodelling and myocardial fibrosis following transcatheter aortic valve implantation compared to surgical aortic valve replacement: a cardiovascular magnetic resonance study. Heart. 2013; 99(16):1185–1191. doi:10.1136/heartjnl-2013-303927. [PubMed: 23749779]
20. Dyverfeldt P, Hope MD, Tseng EE, Saloner D. Magnetic resonance measurement of turbulent kinetic energy for the estimation of irreversible pressure loss in aortic stenosis. JACC Cardiovasc Imaging. 2013; 6(1):64–71. doi:10.1016/j.jcmg.2012.07.017. [PubMed: 23328563]
21. Hope MD, Wrenn J, Sigovan M, Foster E, Tseng EE, Saloner D. Imaging Biomarkers of Aortic Disease. J Am Coll Cardiol. 2012; 60(4):356–357. doi:10.1016/j.jacc.2012.01.072. [PubMed: 22813616]
22. Cecchi E, Giglioli C, Valente S, Lazzeri C, Gensini GF, Abbate R, Mannini L. Role of hemodynamic shear stress in cardiovascular disease. Atherosclerosis. 2011; 214(2):249–256. doi: 10.1016/j.atherosclerosis.2010.09.008. [PubMed: 20970139]
23. Della Corte A, Quarto C, Bancone C, Castaldo C, Di Meglio F, Nurzynska D, De Santo LS, De Feo M, Scardone M, Montagnani S, Cotrufo M. Spatiotemporal patterns of smooth muscle cell changes in ascending aortic dilatation with bicuspid and tricuspid aortic valve stenosis: focus on cell-matrix signaling. J Thorac Cardiovasc Surg. 2008; 135(1):8–18. 18, e11–12. doi:10.1016/j.jtcvs.2007.09.009. [PubMed: 18179910]
24. Rinaudo A, Pasta S. Regional variation of wall shear stress in ascending thoracic aortic aneurysms. Proceedings of the Institution of Mechanical Engineers Part H, Journal of engineering in medicine. 2014; 228(6):627–638. doi:10.1177/0954411914540877.
25. Koullias G, Modak R, Tranquilli M, Korkolis DP, Barash P, Elefteriades JA. Mechanical deterioration underlies malignant behavior of aneurysmal human ascending aorta. J Thorac Cardiovasc Surg. 2005; 130(3):677–683. doi:10.1016/j.jtcvs.2005.02.052. [PubMed: 16153912]
26. Bogren HG, Mohiaddin RH, Kilner PJ, Jimenez-Borreguero LJ, Yang GZ, Firmin DN. Blood Flow Patterns in the Thoracic Aorta Studied with Three-Directional MR Velocity Mapping: The Effects of Age and Coronary Artery Disease. J Magn Reson Imaging. 1997; 7(5):784–793. [PubMed: 9307902]

27. Hope TA, Markl M, Wigstrom L, Alley MT, Miller DC, Herfkens RJ. Comparison of flow patterns in ascending aortic aneurysms and volunteers using four-dimensional magnetic resonance velocity mapping. J Magn Reson Imaging. 2007; 26(6):1471–1479. doi:10.1002/jmri.21082. [PubMed: 17968892]

28. Della Corte A, Bancone C, Conti CA, Votta E, Redaelli A, Del Viscovo L, Cotrufo M. Restricted cusp motion in right-left type of bicuspid aortic valves: a new risk marker for aortopathy. J Thorac Cardiovasc Surg. 2012; 144(2):360–369. 369, e361. doi:10.1016/j.jtcvs.2011.10.014. [PubMed: 22050982]

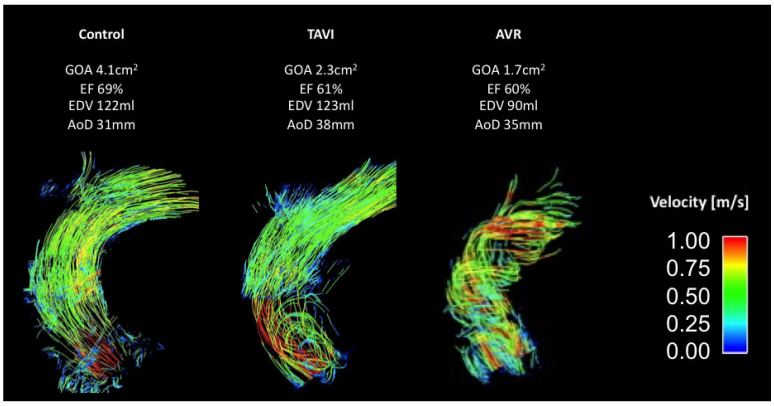

Figure 1.

Representative blood flow patterns in the ascending aorta as illustrated with pathlines (TAVI, transcatheter aortic valve replacement; AVR, aortic valve replacement; EOA, effective orifice area; EF, ejection fraction; EDV, enddiastolic volume; AoD, ascending aortic diameter

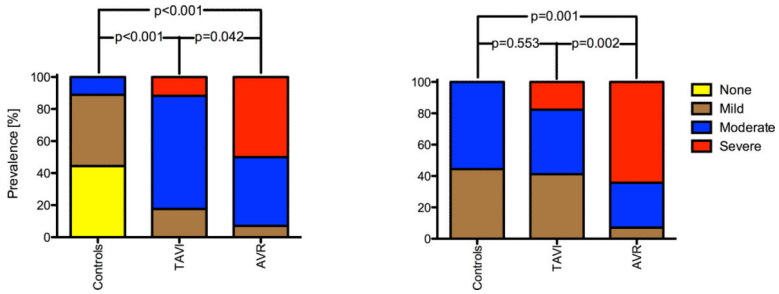

Figure 2.
Comparison of the severity of vortices (left) and helices (right)

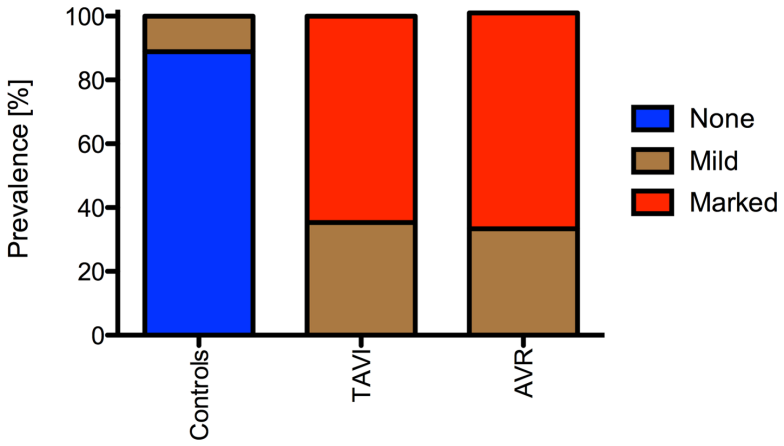

Figure 3.
Prevalence of qualitatively graded blood flow eccentricity.

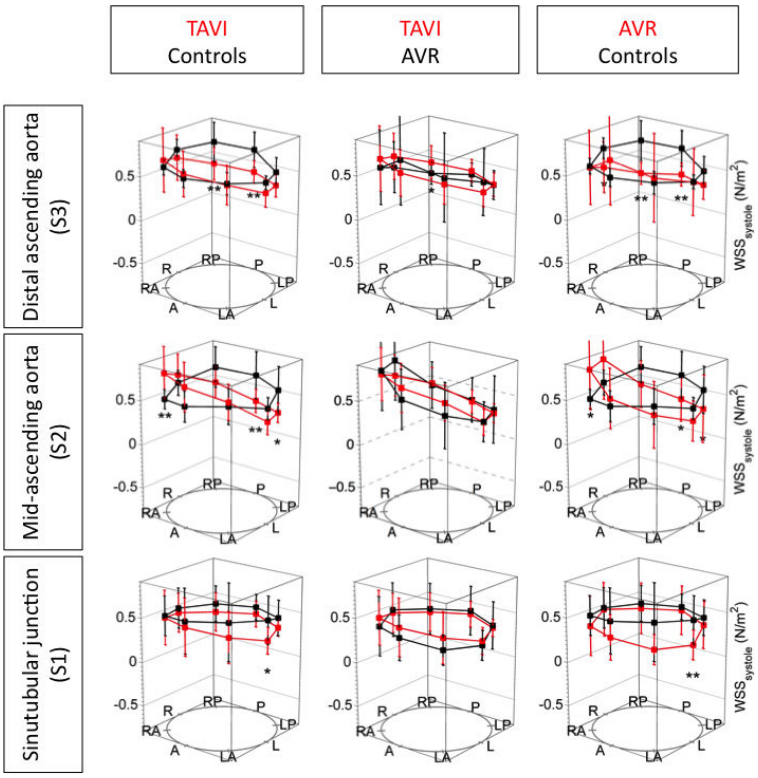

Figure 4.

Distribution of the peak wall shear stress in the ascending aorta. R=right, A=anterior, L=left, P=posterior. * indicates $p < 0.05$ and ** indicates $p < 0.01$

Table 1

Baseline characteristics of the study participants.

Parameter	TAVI	AVR	Controls	p-value
n	17	12	9	---
Sex [females/males]	8/9	4/8	1/8	---
Age [years]	77 ± 7	76 ± 4	55 ± 16	0.001
Prosthetic types	Edwards Sapien XT (n = 17),	Porcine: Medtronic Hancock (n = 4), Labcore (n = 1); Bovine: Edwards Perimount (n = 2), Sorin Mitroflow (n = 2), unknown (n = 3)	---	---
Labeled valve size	25.8 ± 2.2	23.2 ± 2.2	---	0.012
Effective orifice area [cm^2]	1.9 ± 0.3	1.5 ± 0.5	4.0 ± 0.8	< 0.001
Effective orifice area index [cm^2/m^2]	0.9 ± 0.3	0.8 ± 0.2	2.0 ± 0.3	< 0.001
LV* enddiastolic volume [ml]	157.0 ± 63.2	149.9 ± 61.8	139.6 ± 41.4	0.870
LV mass [g|	175.7 ± 59.3	165.2 ± 55.1	129.2 ± 25.3	0.079
LV stroke volume [ml]	87.9 ± 33.1	84.9 ± 32.3	91.4 ± 28.2	0.796
LV ejection fraction [%]	57.2 ± 10.1	58.0 ± 10.9	65.9 ± 6.1	0.038
Ascending aortic diameter [mm]	34.8 ± 3.1	38.5 ± 4.4	30.7 ± 4.8	0.002

Results are given as mean ± standard deviation or as frequencies. The p-values are tested by the Kruskal-Wallis analysis.

*LV, left ventricular